Tuning the perpendicular magnetic anisotropy in tetragonally distorted Fe_xCo_{1-x} alloy films on Rh (001) by varying the alloy composition

F. Luo,[a] X. L. Fu, A. Winkelmann, and M. Przybylski
Max-Planck-Institut für Mikrostrukturphysik, Weinberg 2, 06120 Halle, Germany

(Received 17 October 2007; accepted 14 November 2007; published online 27 December 2007)

Tetragonally distorted Fe_xCo_{1-x} alloy films are grown on Rh (001) showing a strong perpendicular magnetic anisotropy in a wide thickness and composition range. This large perpendicular magnetic anisotropy is chemical composition dependent and reaches a maximum at $x=0.4$. For this composition, we observed an out-of-plane easy axis of magnetization at room temperature with film thickness up to 15 ML. Our experiments show that the proper adjustment of the Fermi level (E_F) by the variation of the Fe_xCo_{1-x} alloy composition and the corresponding tetragonal distortion results in a large perpendicular magnetic anisotropy. © *2007 American Institute of Physics*.
[DOI: 10.1063/1.2821370]

In transition metal films, room temperature perpendicular magnetic anisotropy (PMA) with magnetization perpendicular to the film plane is not only of fundamental interest for magnetism and low dimensional systems but also important for practical applications in high-density perpendicular magnetic recording media.[1,2] In order to further increase the mass data storage density on magnetic hard drives by simply scaling the dimensions of the bits in the storage layer, the perpendicular recording media with a larger PMA are required to prevent the appearance of supermagnetism in smaller isolated single domain grains.[3] Since the mechanisms responsible for PMA have not fully been understood yet, it is important to investigate the microscopic origin of PMA in detail in order to identify potential recording media candidates.

Néel's surface anisotropy, as a consequence of the reduced symmetry at an interface and the enhanced magnetocrystalline anisotropy due to altered electronic structures by interface hybridation, is considered to be the major origin for the observed PMA in Co- or Fe-based ultrathin or multilayer films.[4,5] However, in magnetic systems with a large mismatch between the film and the substrate, it is necessary to also consider the magnetoelastic anisotropy associated with the tensile strain to exactly explain the origin of the PMA in such systems.[6,7] The lattice mismatch induced tetragonal distortion is predicted to reduce the energy separation between the in-plane oriented orbitals (d_{x2-y2} and d_{xy}).[8] Since the magnetic anisotropy energy is inversely proportional to the energy separation between the two levels (d_{x2-y2} and d_{xy}) located below and above the Fermi level (E_F), the PMA therefore is enhanced due to distortion.

From the first-principles calculations, Burkert *et al.*[9] predicted that the uniaxial magnetocrystalline anisotropy (K_u) of bulk Fe_xCo_{1-x} alloys can be tuned not only by tetragonal distortion but also by alloy composition. The maximum K_u is predicted in tetragonally distorted bulk $Fe_{0.4}Co_{0.6}$ alloys with c/a ratio around 1.22. Recently, tetragonally distorted $Fe_{0.4}Co_{0.6}$/Pt (001) (Ref. 10) multilayers with $c/a=1.20$ and 8 ML $Fe_{0.5}Co_{0.5}$ alloy film on Pd (001) (Ref. 11) with $c/a=1.13$ were realized and a largely enhanced PMA was experimentally observed in both cases. Here, we have chosen Fe_xCo_{1-x} alloy films grown on an Rh (001) because this system is a promising candidate for showing a c/a ratio near to a value of 1.22, where the maximum K_u is predicted at a specific alloy composition.[9] In this letter, we find out that the Fe_xCo_{1-x} alloy films on Rh (001) show a room temperature out-of-plane magnetization and keep a strong PMA over a wide thickness and chemical composition range. The Fe_xCo_{1-x} alloy films were grown in a multichamber ultrahigh vacuum system with a base pressure better than 5×10^{-11} mbar and less than 2×10^{-10} mbar during deposition.[11]

Because of the different lattice constants between the thin film and the substrate, large misfit values for fcc Fe (−5.2%) and fcc Co (−6.3%) (Ref. 12) are observed on Rh (001). Since the interlayer lattices of Fe and Co have to be compressed along the c-axis direction while the in-plane lattices have to be expanded to the lattice constant of Rh (001), a perfect layer-by-layer growth is not expected for the Fe_xCo_{1-x} alloy thick films. Figure 1 shows the scanning tunneling microscopy (STM) images of the deposited alloy

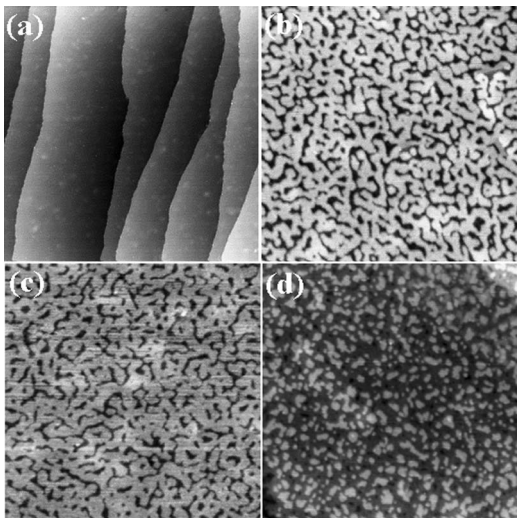

FIG. 1. STM images of (a) Rh (001) with scale 400×400 nm^2; and $Fe_{0.4}Co_{0.6}$ alloy films on Rh with (b) 0.8 ML, (c) 2.9 ML, and (d) 4.2 ML. The scale is 100×100 nm^2.

[a]Author to whom correspondence should be addressed. Paul Scherrer Institut, Villigen PSI, CH-5232, Switzerland. Tel.: +41 56 3104519. FAX: +41 56 3102646. Electronic mail: feng.luo@psi.ch.

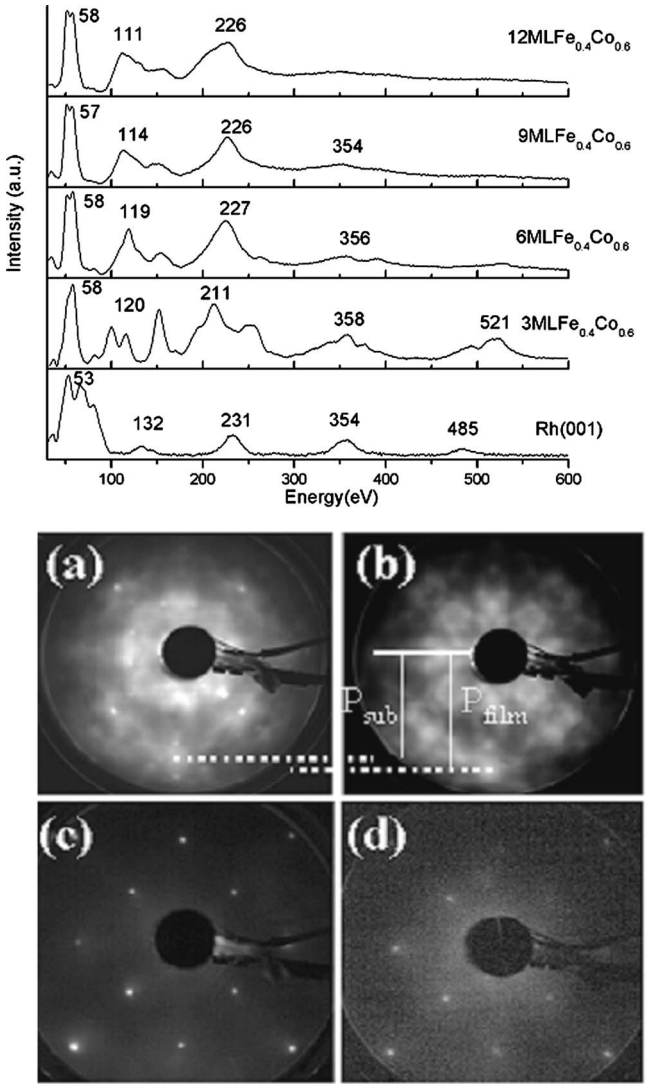

FIG. 2. LEED $I(E)$ curve of the (0, 0) spot as a function of incident electron energy on Rh (001) as well as $Fe_{0.4}Co_{0.6}$ alloy films with different thicknesses. The lower panel shows the Kikuchi patterns of (a) Rh (001) and (b) 7 ML $Fe_{0.4}Co_{0.6}$, combined with LEED patterns of (c) Rh (001) and (d) 7 ML $Fe_{0.4}Co_{0.6}$.

films with different film thicknesses on the Rh substrate. From Figs. 1(b)–1(d), it is clear that the lay-by-layer growth of the $Fe_{0.4}Co_{0.6}$ film on Rh (001) persists up to 3 ML and then changes to three-dimensional growth mode when the film thickness increases, which is confirmed by high energy electron diffraction oscillations persisting up to 3 ML (not shown). This growth mode is similar to that on Pd (001). Meanwhile, we also found that the surface morphology as well as the spot positions in the low energy electron diffraction (LEED) patterns are not sensitive to the variation of alloy composition.

From the spot analysis of the LEED patterns, we can confirm that the alloy films still grow in a partially pseudomorphic mode until 10 ML and the in-plane lattice constant of the ordered film is thus determined to have the same value as the substrate. In order to address the crystallographic structure of $Fe_{0.4}Co_{0.6}$ alloy film on Rh (001) along the surface normal, LEED $I(E)$ curves of the specular (0, 0) spot were recorded, as shown in Fig. 2. Analyzed by a kinematic approach, the average interlayer spacing d is determined by the energetic positions E_n of the Bragg maxima. Here, d is obtained from a linear regression of an E_n versus n^2 plot by applying the relation $E_n = h^2 n^2/(8m_e \cos^2 \alpha d^2) + V_0$, where h, m_e, and α denote Planck's constant, electron mass, and incidence angle relative to the sample normal, respectively. For E_n, we simply used the energies of the maximum peak intensity. The calculated interlayer space d above 3 ML is around 0.33 nm and keeps stable until 9 ML. Above 12 ML, the LEED spot is too weak and the calculated data are unreliable. For the $Fe_{0.4}Co_{0.6}$ alloy films with thicknesses from 3 to 9 ML, the corresponding c/a ratio is 1.23 ± 0.03. The Kikuchi patterns obtained in the LEED apparatus at 1 keV also allowed us to estimate the c/a ratio of the films, because they are providing instantaneous real-space information on the local order of the crystal structure. The quasielastically backscattered electrons can be thought to be emitted from point like sources inside the crystal and are then predominantly scattered in the forward direction by the surrounding atoms on their way out of the sample. In this way, interatomic scattering directions show up as intensity maxima. The distortion of a crystal therefore can be obtained from the position shift of the intensity maxima.[11] Figures 2(a) and 2(b) show the Kikuchi patterns of the clean Rh (001) and of a 7 ML $Fe_{0.4}Co_{0.6}$ alloy film. A clear change of the position of intensity maxima marked as lines in the Kikuchi patterns from the substrate and the 7 ML grown film is observed, which indicates that the alloy film is distorted. The corresponding LEED patterns are shown in Figs. 2(c) and 2(d). The LEED pattern of the alloy films keeps the same spot position compared to that of the clean Rh substrate, confirming that the in-plane lattice constant of the 7 ML ordered film is the same as that of the substrate. From the inset of Figs. 2(a) and 2(b), we measured the distances P_{film} and P_{sub} between the center position of the Kikuchi patterns and the forward scattering maxima position of alloy film and substrate, respectively. The tetragonal distortion is calculated from the scattering angles corresponding to P_{film} and P_{sub}, which are determined from a calibration of the LEED screen by the known energy-dependent position of LEED spots from the Rh (001) substrate. This gave the c/a ratio of 1.24 ± 0.04 for the 7 ML thick $Fe_{0.4}Co_{0.6}$ film on Rh (001), consistent with our analysis of the LEED $I(E)$ curves. There is no clear difference in the Kikuchi patterns from 7 ML Fe_xCo_{1-x} alloy films with changing alloy composition. For the investigated films ($0.3 < x < 0.7$), the c/a ratio is not sensitive to the Co content and keeps constant as observed from Kikuchi patterns from films of different alloy compositions.

We measured thickness dependent hysteresis loops in longitudinal and polar geometry by *in situ* magneto-optical Kerr effect (MOKE) at room temperature on ultrathin films grown as wedges on Rh (001) and Pd (001). No polar MOKE signal was detected for pure Co and Fe films on Rh (001) system at room temperature in the thickness range up to 15 ML. At the composition $0.3 < x < 0.7$, it showed a clear out-of-plane easy axis of magnetization below certain thickness point, which is also composition dependent. Figure 3 shows typical polar loops of $Fe_{0.4}Co_{0.6}$ with different film thicknesses. Up to 15 ML, the remanent polar signal equals the saturation signal, indicating that the remanent magnetization of the film is pointing out of plane. Above this thickness, the remanent polar signal gradually disappears and the remanent longitudinal Kerr signal appears. This spin reorientation transition (SRT) thickness is defined as d_c. Below d_c, due to tetragonal distortion, the K_u of the distorted alloy

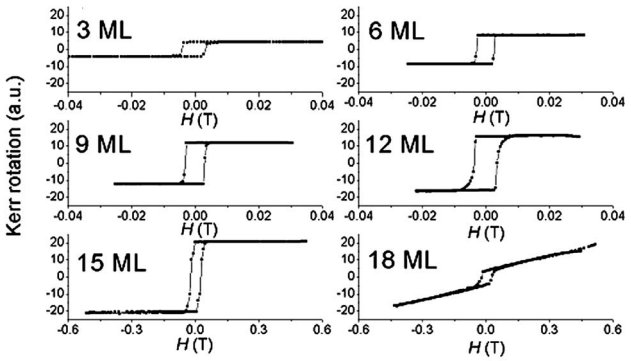

FIG. 3. Series of polar MOKE loops of $Fe_{0.4}Co_{0.6}$ alloy films on Rh (001) with different thicknesses measured at room temperature.

films is higher than the shape anisotropy of alloy films, showing out-of-plane spontaneous magnetization. With increasing thickness of the alloy film, the appearance of lattice defects will reduce the strain originating from the large lattice mismatch between Rh and alloy films. This is also confirmed by the gradual disappearance of LEED patterns for the thicker films. The K_u of the film is decreased by releasing the film strain[11] and cannot overcome the shape anisotropy, leading to a SRT from out of plane to in plane.

In Fig. 4(a), we show how the thickness d_c depends on the film composition for alloy films on Rh (001) and Pd (001). Since the pure Fe and Co films grown on Pd (001) and Rh (001) are spontaneously magnetized in plane, it is reasonable to assume that the surface and interface anisotropies do not contribute significantly to the PMA in both of these two systems. Since the saturation magnetization of Fe_xCo_{1-x} alloy films slightly increases with increasing Fe content and then decreases when $x>0.8$,[9] the shape anisotropy is therefore only slightly dependent on the composition. In such a situation, we can take d_c as a direct indication of the volume magnetocrystalline anisotropy (Kv) and hence the Ku. It is clear that the d_c of Fe_xCo_{1-x} alloy films on Rh (001) increases with alloy composition x and reaches a maximum at x equal to 0.4 and then decreases when the Fe content still increases. We can expect that the K_u follows the same trend. This composition dependent K_u is consistent with the theoretical calculations.[9] At room temperature, Fe_xCo_{1-x} alloy

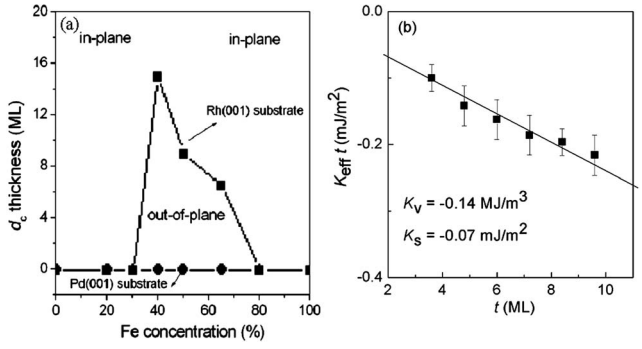

FIG. 4. (a) Regions of perpendicular and in-plane easy axis of magnetization measured at room temperature for Fe_xCo_{1-x} alloys at room temperature grown on Pd (001) and Rh (001), respectively. (b) The K_{eff} of $Fe_{0.5}Co_{0.5}$ alloy film grown on Pd (001) as a function of film thickness.

films on Pd show in-plane magnetization at all Fe compositions. When the samples are cooled down to 70 K, the films show out-of-plane magnetization at x equal to 0.5,[11] which indicates that the $Fe_{0.5}Co_{0.5}$ alloy film has the largest K_u. Considering that the shape anisotropy is a constant and has no obvious difference when $Fe_{0.5}Co_{0.5}$ alloy film is grown on Pd and Rh substrates, the K_u of $Fe_{0.5}Co_{0.5}$ on Pd (showing in-plane easy magnetization axis) is therefore smaller than that on Rh (001) (showing out-of-plane easy magnetization axis) at room temperature. When the c/a ratio is changed from 1.13 [11] to 1.24, the K_u is expected to increase according to the theoretical calculations.[9] From Fig. 4(a), it can be concluded that both a specific tetragonal distortion and proper alloy composition are necessary to get the largest PMA on Rh (001). In this distorted system, the tetragonal distortion lifts the degeneracy of $3d$ orbital levels[8] and reduces the energy separation between the d_{x2-y2} and d_{xy} states. The K_u is inversely proportional to the energy separation between the electronic levels located below and above E_F. K_u then is expected to change drastically when E_F is moving by varying the number of valence electrons.[8] By properly selecting the alloy concentration, the E_F can be tuned to obtain a large K_u.

Combined with the longitudinal and polar MOKE measurements, we can get the effective magnetic anisotropy energy (K_{eff}) by measuring the field H_A needed to saturate the magnetization in the hard direction. Based on the formula $K_{\text{eff}}=K_v+(K_s+K_i)/t$, we plot the $K_{\text{eff}}t$ as a function of t for $Fe_{0.5}Co_{0.5}$ on Pd (001) shown in Fig. 4(b). Here, the K_s and K_i are the surface and interface anisotropy, and t is the film thickness. From the linear fit of $K_{\text{eff}}t$ below 10 ML, the subtracted K_v is -0.14 MJ/m^3 (-12 μeV/atom) and the K_s+K_i is -0.07 mJ/m^2. Since the shape energy is a constant of -120 μeV/atom (an average magnetization of $2.0\mu_B$/atom and c/a is 1.13), the calculated K_u is around 108 μeV/atom, which is consistent with the theoretical calculated K_u ($\sim$200 μeV/atom).[9] Unfortunately, it was impossible to saturate the Fe_xCo_{1-x} alloy films on Rh (001) in plane within the available field in our MOKE setup, thus it was impossible to calculate anisotropy constants for this system.

[1] P. F. Carcia, A. D. Meinholdt, and A. Suna, Appl. Phys. Lett. **47**, 178 (1985).
[2] T. Suzuki, Scr. Metall. Mater. **33**, 1609 (1995).
[3] D. Weller, A. Moser, L. Folks, M. E. Best, W. Lee, M. F. Toney, M. Schwickert, J. U. Thiele, and M. F. Doerner, IEEE Trans. Magn. **36**, 10 (2000).
[4] F. J. A. den Broeder, D. Kuiper, A. P. van de Mosselaer, and W. Hoving, Phys. Rev. Lett. **60**, 2769 (1988).
[5] Y. Wu, J. Stöhr, B. D. Hermsmeier, M. G. Samant, and D. Weller, Phys. Rev. Lett. **69**, 2307 (1992).
[6] D. Sander, Rep. Prog. Phys. **62**, 809 (1999).
[7] B. Schulz and K. Baberschke, Phys. Rev. B **50**, 13467 (1994).
[8] P. Bruno, Phys. Rev. B **39**, 865 (1989).
[9] T. Burkert, L. Nordström, O. Eriksson, and O. Heinonen, Phys. Rev. Lett. **93**, 027203 (2004).
[10] G. Andersson, T. Burkert, P. Warnicke, M. Björck, B. Sanyal, C. Chacon, C. Zlotea, L. Nordström, P. Nordblad, and O. Eriksson, Phys. Rev. Lett. **96**, 037205 (2006).
[11] A. Winkelmann, M. Przybylski, F. Luo, Y. S. Shi, and J. Barthel, Phys. Rev. Lett. **96**, 257205 (2006).
[12] U. Gradmann, *Handbook of Magnetic Materials* (Elsevier, New York, 1993), Vol. 7, p. 1.